Vol. 578: 99–114, 2017
https://doi.org/10.3354/meps12252

MARINE ECOLOGY PROGRESS SERIES
Mar Ecol Prog Ser

Published August 31

Aggregation, Allee effects and critical thresholds for the management of the crown-of-thorns starfish *Acanthaster planci*

Jacob G. D. Rogers[1,*], Éva E. Pláganyi[2], Russell C. Babcock[2]

[1]School of Mathematics and Physics, University of Queensland, Brisbane 4072, Queensland, Australia
[2]CSIRO Oceans and Atmosphere, Brisbane 4072, Queensland, Australia

ABSTRACT: We investigated how density and aggregation influence crown-of-thorns starfish *Acanthaster planci* reproductive success, using an empirically-tuned, individual-based simulation model that incorporates spatial and temporal biological stochasticity associated with spawning, and a kinetics model of fertilisation that explicitly incorporates the probability of polyspermy. Greater aggregation of individuals relieved Allee fertilisation dynamics, particularly at low densities, leading to higher rates of successful monospermic fertilisation and allowing populations to produce many more zygotes. This is likely more important to smaller, rather than larger, populations, due to limited and more variable reproductive success. In higher density populations a fertilisation optimum was observed at moderate levels of aggregation, above which monospermic fertilisation plateaued or even declined. This was likely due to 2 factors: the spatial dynamics of gamete plume dispersal and polyspermic fertilisation. Comparison of *in situ* natural spawning aggregation with model results indicates a cost-benefit equilibrium may exist between aggregation and reproductive success, and that relief from mechanisms limiting aggregation (for example, decreased relative predator abundance) may permit increased aggregation resulting in greater fertilisation and zygote production. We propose an Allee threshold of 3 starfish ha^{-1} (for starfish of a mean diameter 345 mm), below which reproductive capacity is greatly reduced regardless of aggregation level. These preliminary findings posit aggregation as a key factor in outbreak formation that may feasibly be incorporated into preventative management strategies to detect and define incipient outbreak conditions and to mitigate subsequent risk.

KEY WORDS: COTS · Spawning · Fertilisation · Polyspermy · Pest management · Marine invertebrate · Coral

INTRODUCTION

Acanthaster planci (the crown-of-thorns starfish) is a corallivorous free-spawning asteroid that periodically undergoes extensive population increases (outbreaks) that can cause widespread loss of coral cover to reefs of the Indo-Pacific (Sweatman et al. 2011, Nakamura et al. 2014, Pratchett et al. 2014). Between 1985 and 2012, *A. planci* constituted the second largest cause of coral loss on the Great Barrier Reef (GBR), accounting for 42% of the estimated 50.7% loss of coral cover (De'ath et al. 2012). The mechanisms suspected to govern the occurrence of outbreaks have been modelled frequently and include predator removal, hydrography, and eutrophication (Dulvy et al. 2004, Brodie et al. 2005, Fabricius et al. 2010, Wooldridge & Brodie 2015), though no single cause has been conclusively demonstrated.

It has also been proposed that outbreaks are a natural feature of *A. planci* reproductive biology, arising from increased fertilisation and larval recruitment stemming from aggregations of spawning individu-

*Corresponding author: jacob.rogers1@uqconnect.edu.au

als (Dana et al. 1972, Vine 1973). It is known that a combination of strong coral prey preferences (Pratchett 2007, Kenyon & Aeby 2009), chemo-attractants (Ormond et al. 1973, Teruya et al. 2001), and searching behaviour derived from food limitation (Weber & Woodhead 1970, Keesing & Lucas 1992) can catalyse aggregations. Within such aggregating populations, or more generally within high density populations, fertilisation efficiency and larval recruitment could be significantly amplified as in other marine free-spawners (Levitan & Young 1995, Lundquist & Botsford 2004, 2010). Individual starfish are capable of fertilisation even when separated by large distances (Babcock et al. 1994). However, the role of aggregation and population density in the reproductive success of *A. planci* is not well understood, nor quantified, and is a major gap in our efforts to control outbreaks. Increased reproductive success could potentially precipitate outbreaks (Dana et al. 1972, Vine 1973, Birkeland & Lucas 1990) and understanding the quantitative effect of spawner aggregation — the extent of Allee dynamics — will therefore allow more rigorous evaluation of the mechanisms thought to trigger outbreaks and potentially reveal options for controlling them.

Population density and Allee dynamics have been the subject of numerous ecological and fisheries management models for marine free-spawning invertebrates (Babcock et al. 1994, 2014, Claereboudt 1999, Hobday & Tegner 2002, Lundquist & Botsford 2004, 2010). The majority of these models simulate gamete dispersion through turbulent diffusion, calculating fertilisation success and larval production as a function of gamete properties, fertilisation kinetics, and conspecific spatial concentrations (Babcock et al. 1994, 2014, Levitan & Young 1995, Claereboudt 1999). Empirical exploration of Allee effects on reproductive success in free-spawning marine invertebrates has revealed that increasing inter-spawner distance, such as at reduced spawner density, may result in reproductive collapse whereby a population cannot sustain itself below a certain threshold (Quinn et al. 1993, Lundquist & Botsford 2010). This is illustrated through Allee dynamics having contributed to a number of fishery declines due to exploitation-mediated recruitment failure (reviewed by Liermann & Hilborn 2001) and bringing some species close to extinction (e.g. white abalone; Hobday et al. 2000, Stierhoff et al. 2012). Within the context of free-spawning invertebrates, Allee fertilisation manifests as reduced efficiency at low densities leading to suppressed larval production (Lundquist & Botsford 2004, 2010). This may be overcome to some extent by aggregation of spawning individuals (Pennington 1985, Levitan & Petersen 1995); however, there may be limits to the benefits of high density (and high levels of aggregation) since polyspermy may counteract the benefits of increased sperm concentrations (Levitan 2004).

Currently, understanding of *A. planci* aggregative behaviour is largely based upon small-scale experimental studies (Babcock & Mundy 1992, Babcock et al. 1994) and inferences drawn from other free-spawning species (Pennington 1985, Levitan & Young 1995, Lundquist & Botsford 2010). However, significant research into the species' reproductive biology has revealed 2 key distinguishing features (e.g. Kettle & Lucas 1987, Birkeland & Lucas 1990, Benzie et al. 1994, Benzie & Dixon 1994). The first is that large female *A. planci* are able to spawn >60 to 100 million eggs during a single spawning season (Kettle & Lucas 1987, Birkeland & Lucas 1990, Babcock et al. 2016) with male gamete production similarly prolific (Babcock et al. 2016). The second feature is that fertilisation rates of *A. planci* were found to be >20% at a distance of 64 m downstream from a single spawning male (Babcock & Mundy 1992). This far exceeds the fertilisation rates in other marine free-spawners such as *Strongylocentrotus droebachiensis* (green sea urchin), which requires distances <1 m to achieve effective fertilisation (Pennington 1985). The quantity of gametes released during spawning and the extensive distances at which fertilisation is effective suggests that the effect of population density and aggregative behaviour may operate at quite different scales in the reproductive success of *A. planci* than in other free-spawning invertebrates.

The number of gametes *A. planci* is able to spawn is limited through size-based fecundity (Babcock et al. 1994, 2016). Moreover, female *A. planci* egg production is reported to increase by >50 million eggs yr^{-1} as individual size increased from <300 to 400 mm diameter (Pratchett et al. 2014). Reproductive dynamics are therefore likely to be sensitive to the size of spawning *A. planci*, as size influences gamete availability in the population. Understanding how reproductive capacity changes in response to mean diameter of a population may be used in conjunction with growth rates to provide a time frame within which management can act.

Allee mechanisms such as fertilisation efficiency and aggregation in free-spawning invertebrates have the capacity to limit population reproductive potential (Liermann & Hilborn 2001, Tobin et al. 2011). Hence, quantifying the effect of spawner aggregation and Allee fertilisation is essential to better

understand *A. planci* reproductive dynamics and manage the species' risk of outbreak by keeping population density and/or aggregations below some Allee threshold. Here, we investigated how density and aggregative behaviour accentuates *A. planci* population reproductive efficiency and total reproductive output through reducing sperm limitation and Allee fertilisation effects. Specifically, we implemented a spatially-explicit empirical fertilisation kinetics model, including polyspermic fertilisation, to quantitatively estimate population-level larval production and monospermic fertilisation success as a function of (1) population density and (2) aggregation, and (3) compared results with *in situ* measurements of *A. planci* population aggregation. It is demonstrated that optimal aggregative behaviour can mitigate Allee dynamics and that *A. planci* behaviour reflects this, and also that polyspermy may limit the benefits to individuals of aggregative behaviour even at relatively low densities.

METHODS

An individual-based simulation approach was implemented to incorporate spatial and temporal biological stochasticity associated with various realisations of *A. planci* spatial distributions and demographic factors. Spawner location and demographics were generated through an aggregation model based upon a clustering algorithm. Gamete dispersion from each spawner was modelled as a diffusive process with zygote production and fertilisation efficiency computed via gamete properties, fertilisation kinetics, starfish density, and spatial distribution. The diffusion and fertilisation models are respectively based upon those of Babcock et al. (2014) and Millar & Anderson (2003), and tuned to empirical data collated from the literature (Babcock et al. 1994). Parameters and their values are summarised in Tables 1–3.

Model configuration

To calculate the diffusion of gametes under a given set of parameters, a focal region of distance 100 m in the cross-stream direction and 100 m in the direction of current is considered in water of depth 7 m. As *A. planci* gametes are capable of large scale dispersal (Babcock et al. 1994), it is necessary to account for gametes (eggs and sperm) originating from individuals outside the focal region. These boundary conditions are modelled by explicitly simulating neighbouring regions such that the focal region is centred on the downstream boundary of a domain measuring 200 m in the cross-stream direction by 300 m in the direction of current (6 ha). This allows gamete diffusion and turbulent dispersion at larger scales to be incorporated. Unidirectional flow is assumed, therefore downstream spawning would have no effect on the focal area and is not included. The total spatial configuration spans 200 × 300 m by 7 m deep, discretised into 0.5 × 0.5 × 0.5 m cubic cells (3.36×10^6 cubic cells in total).

Aggregation model

Aggregation represents increased abundance of individuals within finite subregions of the model. To investigate the effect of aggregative behaviour on the reproductive success of *A. planci*, a marked spatial cluster process is employed. A cluster process involves a point process — a characterisation of the random distribution of cluster 'centres' in space — each of which is associated with a finite set of random points whose superposition is termed a cluster process (Baddeley 2007). Here, the parent process entails sampling a fraction ($0 < \alpha \leq 1$) of the total number of starfish (N) from a bivariate uniform distribution over the substratum of the model. These form the cluster centres. To each centre, a random number

Table 1. Summary of aggregation model parameters, values and sources

Parameter	Description	Value (units)	Source
α	Cluster proportionality constant	0.15 (unitless)	
β^*	Cluster-density proportionality constant	0–1 (unitless)	
ξ	*Acanthaster planci* maximal diameter	Sampled from distribution (mm)	
R	Nearest neighbour index	Computed (unitless)	Krebs (1999)
r_A	Nearest neighbour distance	Computed (m)	Krebs (1999)
N	Individuals simulated	0–300 (count)	
A	Total model area	60000 (m^2)	Babcock et al. (2014)
L	Model perimeter	1000 (m)	Babcock et al. (2014)

Table 2. Summary of diffusion model parameters, values and sources

Parameter	Description	Value (units)	Source
x	Distance parallel to current (i.e. downstream distance)	Assigned (m)	Babcock et al. (1994)
y	Distance horizontal to current (i.e. cross-stream distance)	Assigned (m)	Babcock et al. (1994)
z	Distance vertical to current	Assigned (m)	Babcock et al. (1994)
P_m	Proportion of male gonad spawned	0.33 (unitless)	Babcock et al. (1994)
P_f	Proportion of female gonad spawned	0.50 (unitless)	R. C. Babcock (unpubl. data)
V_m	Volumetric sperm density[a]	5.23×10^{10} (sperm g^{-1})	R. C. Babcock (unpubl. data)
V_f	Volumetric egg density[a]	9×10^4 (eggs g^{-1})	Babcock et al. (1994)
T_s	Duration of spawning[b]	2700 (s)	Babcock et al. (1994), Benzie et al. (1994)
S	Sperm concentration	Computed (sperm m^{-3})	Babcock et al. (1994)
E	Egg concentration	Computed (eggs m^{-3})	Babcock et al. (1994)
Q_s	Sperm release rate	Computed (sperm s^{-1})	
Q_e	Egg release rate	Computed (eggs s^{-1})	
U	Mean current velocity	0.12 (m s^{-1})	Babcock et al. (1994)
Δt	Gamete cell transient time	Computed (s)	
Δd	Gamete horizontal downstream advection distance during Δt	0.5 (m)	
h	Height of gamete release	0.5 (m)	Babcock et al. (1994)
D	Water column depth	7 (m)	Babcock et al. (2014)
κ	Plume diffusivity rate	0.55 (unitless)	
u	Friction velocity	0.1 U (m s^{-1})	Babcock et al. (2014)
σ_y, σ_z	Spatial standard deviation of diffusion in y-, z-axis	Computed (unitless)	Babcock et al. (1994)
α_y	Diffusion coefficient for y-axis	8.61 (unitless)	
α_z	Diffusion coefficient for z-axis	0.51 (unitless)	

[a]Diluted gamete concentrations under the assumption of neutral buoyancy
[b]Gametes shed at constant rate over duration of spawning

Table 3. Summary of fertilisation model parameters, values and sources

Parameter	Description	Value (units)	Source
$P^{F}_{t_c}$	Total fertilisation	To be solved (%)	Vogel et al. (1982)
$P^{M}_{t_c}$	Monospermic fertilisation	To be solved (%)	Millar & Anderson (2003)
$P^{P}_{t_c}$	Polyspermic fertilisation	To be solved (%)	Millar & Anderson (2003)
Z	Zygote production	To be solved (zygotes)	Babcock et al. (2014)
t_c	Sperm–egg contact time	equal to Δt (s)	
u_s	Sperm swimming speed	1.9×10^{-4} (m s^{-1})	Levitan et al. (1991)
β_0	Sperm–egg collision rate	3.8×10^{-8} (m^2 s^{-1})	
β	Fertilisation rate constant	9.42×10^{-10} (3% egg cross sectional area – rate in enclosed vessel; m^2 s^{-1})	Babcock et al. (1994)
S_t	Sperm concentration after time t of egg exposure at location	Computed (sperm m^{-3})	Vogel et al. (1982)
P_s	Proportion of population spawning	0.68 (max; unitless)	Babcock et al. (1994)
S_r	Sex ratio	1:1 (males to females)	Babcock et al. (2014)
T_v	Duration of gamete viability	7200 (s)	Benzie & Dixon (1994)

of Cartesian distances are sampled from the parent distribution, ensuring each displacement (individuals' locations) is within the model and that population density is satisfied. A fraction of each distance ($0 < \beta^* \leq 1$) is taken, such that points tend towards the centre as $\beta^* \rightarrow 0$. Hence, parameter values of $\alpha = 1$ and $\beta^* = 1$ will result in a completely random spatial distribution, whilst taking $\alpha \rightarrow 0$ and $\beta^* \rightarrow 0$ will yield increasingly aggregated distributions. Each individual is independently marked with a gender (equal sex

ratio), whether or not they participate in the spawning event (maximum of 68%; Babcock et al. 1994), and a size diameter ξ (mm; sampled from distribution with mean 345 mm; see Fig. S1 in the Supplement at www.int-res.com/articles/suppl/m578p099_supp.pdf) (Pratchett 2005). The degree to which individuals are aggregated is measured through a modified boundary-corrected nearest neighbour analysis.

Nearest neighbour analysis measures the deviation of an observed spatial pattern from a random pattern (Clark & Evans 1954). The deviation is indexed by the value R, and the analysis modified such that if the observed pattern is random, $R = 0$ and tends towards 1 if aggregation is present. Conversely, R approaches a value of ca. −2.15 if the spatial distribution is regular. Correction of the boundary accounts for starfish located near the boundary experiencing comparatively larger nearest neighbour distances than those closer to the centre (Krebs 1999). Without correction, a bias favouring regular distributions would be present. The analysis considers the nearest neighbour distance, r_A (m), averaged over N individuals within a spatial region of surface A (m^2) and perimeter L (m). R is given by:

$$R = 1 - \frac{\sum_N r_A}{N}\left(\frac{1}{2}\sqrt{\frac{A}{N}} + \left(0.051 + \frac{0.041}{\sqrt{N}}\right)\left(\frac{L}{N}\right)\right) \quad (1)$$

Diffusion model

The shedding of gametes into a flow is modelled as a plume diffusion problem (advection–diffusion problem under a steady state assumption). The model was selected for its simple implementation and reflection of the experimental conditions under which data — to which the model is subsequently tuned — were measured (Babcock et al. 1994). Water moves at a mean velocity of U (m s^{-1}) aligned with the positive x-axis and each individual is considered to be a point source located an equal distance, h (m), above a benthic boundary layer. Topographic variation above the boundary layer (resulting in perturbation to the flow structure) is assumed to be negligible. The movement of gametes principally occurs along the x-axis in the direction of current and it is assumed that the current velocity is of sufficient magnitude that gamete dispersal along the x-axis is solely due to advection (i.e. advection greatly exceeds diffusion). The dispersive effect of eddy diffusivity is taken to be strictly a function of downstream distance from a spawner due to increasing dispersal with increased downstream displacement. Surface reflection is modelled via the addition of a mirror source above the sea surface boundary such that any gametes that diffuse to the surface are reflected back into the flow. Similarly, gametes are assumed to not penetrate the benthic boundary layer. Under these assumptions, gametes are thoroughly mixed by turbulence to produce downstream plumes of spawning individuals (Denny & Shibata 1989). Isotropic diffusivity is not assumed. For individuals of diameter ξ, male and female gonad weights are given by empirical size–fecundity relationships (Babcock et al. 2016) from which sperm and eggs are derived to be shed into the flow at rates Q_s (sperm s^{-1}) and Q_e (eggs s^{-1}), respectively. Under these assumptions, gametes are thoroughly mixed by turbulence to produce downstream plumes of spawning individuals (Denny & Shibata 1989). Emission rates are given by:

$$Q_s(\xi) = \frac{P_m V_m (1.9977e^{0.0177\xi})}{T_s} \quad (2)$$

$$Q_e(\xi) = \frac{P_f V_f (4.7431e^{0.0106\xi})}{T_s} \quad (3)$$

where T_s is the spawning duration (s), P_i the proportion of gonad spawned, and V_i the volumetric gamete density (gametes g^{-1}), with subscript 'i' denoting reference to male (m) or female (f) individuals. T_s is discretised into temporal elements of length Δt (s) which allows for their dynamics to be evaluated as a function of time-dependent conditions (Zannetti 1990) — namely the transport of free sperm and unfertilised eggs downstream of a spawner (i.e. omitting already fertilised eggs and sperm lost due to egg adhesion). The distance gametes advect horizontally downstream during each temporal element, Δd (m), is taken equal to the resolution of the model in the direction of current (0.5 m). Therefore, for a given current velocity, U (m s^{-1}), the required temporal element length, Δt, is calculated to be:

$$\Delta t = \frac{\Delta d}{U} \quad (4)$$

The temporal element length (Δt = 4.17 s) reflects the time sperm and eggs interact at a given spatial location and is subsequently used as the time over which fertilisation occurs at each point in the model configuration. Consequently, the steady state sperm concentration, S, and egg concentration, E, in a water column of depth D at distance (x,y,z) from a spawner of diameter ξ is given by:

$$S(x,y,z) = \frac{Q_s(\xi)}{2\pi U \sigma_y \sigma_z} e^{\frac{-y^2}{2\sigma_y^2}} \left(e^{\frac{-(z+h)^2}{2\sigma_z^2}} + e^{\frac{-(z-h)^2}{2\sigma_z^2}} + e^{\frac{-(2D-z-h)^2}{2\sigma_z^2}} \right) \quad (5)$$

$$E(x,y,z) = \frac{Q_e(\xi)}{2\pi U\sigma_y\sigma_z} e^{\frac{-y^2}{2\sigma_y^2}} \left(e^{\frac{-(z+h)^2}{2\sigma_z^2}} + e^{\frac{-(z-h)^2}{2\sigma_z^2}} + e^{\frac{-(2D-z-h)^2}{2\sigma_z^2}} \right) \quad (6)$$

where the spatial standard deviations are modelled by:

$$\sigma_y = \alpha_y(u / U)x^{\kappa} \quad (7)$$

$$\sigma_z = \alpha_z(u / U)x^{\kappa} \quad (8)$$

The steady state equations (Eqs. 5 & 6) model the gamete concentration distribution downstream of an individual spawning indefinitely at a constant rate. Empirical measures and numerical simulations have shown that both *A. planci* sperm and eggs can be treated as passive and neutrally buoyant particles (Benzie et al. 1994). Thus, inclusion of terms describing particle deposition and settling (Stockie 2011) are omitted. Diffusion parameters α_y and α_z are determined empirically and characterise the shape of the plume, whilst κ describes the rate of growth of the dispersive effect of eddies on the plume. The friction velocity, u (m s^{-1}), accounts for the distance a particle is displaced as a result of turbulent eddies over a small period of time, and is taken as a fraction (0.10) of the mean current velocity U (m s^{-1}). Turbulence intensity is measured as a function of Reynold's shear stress and is expressed as u / U which reduces to a dimensionless constant (0.10).

Fertilisation kinetics model

Here, we develop a kinetics model of fertilisation that explicitly incorporates the probability of polyspermy (Millar & Anderson 2003). Fertilisation (both mono- and polyspermic) is calculated at each of the cubic cell vertices (x,y,z) as a function of the sperm and egg concentrations there. The model assumes that sperm attach to the first egg they encounter regardless of whether the egg has been fertilised or not ('Don Ottavio' model of fertilisation; Vogel et al. 1982). Fertilisation rates are estimated through calculating the probability of a sperm and egg colliding within a turbulent flow by observing collisions over a contact time t_c (s). If t_c exceeds the viability of gametes, T_v (s), then t_c should be replaced with T_v such that collisions are observed over the period where sperm are viable (Millar & Anderson 2003). The contact time is taken equal to the advection time of eggs through model cells (i.e. each temporal element; $t_c = \Delta t$). At each point in the spatial domain, the initial concentration of free sperm and unfertilised eggs (m^{-3}) are denoted by S_0 and E_0, respectively. The rate of sperm–egg collisions is denoted by the parameter β_0 and is defined to be the volumetric flow rate of sperm through the cross section of an egg. The collision rate is computed through multiplication of the cross-section of an *A. planci* egg (diameter: 2 × 10^{-4} m; Babcock et al. 1994) by sperm swimming speed, u_s (1.9 × 10^{-4} m s^{-1}; Levitan et al. 1991). Consequently, under the Don Ottavio model of fertilisation, the sperm concentration, S_{t_c}, after exposure to an egg concentration, E_0, for time t_c is given by:

$$S_{t_c} = S_0 e^{(-\beta_0 E_0 t_c)} \quad (9)$$

from which the number of sperm lost due to adhesion to eggs, $S_{Reduction}$, can be deduced to be

$$S_{Reduction} = S_0 - S_{t_c} = S_0(1 - e^{(-\beta_0 E_0 t_c)}) \quad (10)$$

Defining β as the fertilisation rate constant equal to the egg surface area receptive to fertilisation (3%, rate in an enclosed vessel; Babcock et al. 1994) yields the mean number of sperm attachments resulting in fertilisation by time t_c as:

$$x(t_c) = \frac{\beta S_0}{\beta_0 E_0}(1 - e^{-\beta_0 E_0 t_c}) \quad (11)$$

Assuming the arrival of fertilising sperm on an egg are Poisson-distributed (Millar & Anderson 2003), the probability an egg is fertilised by at least one sperm, $P^F_{t_c}$, at the point (x,y,z) by time t_c is:

$$P^F_{t_c}(x,y,z) = 1 - e^{-x(t_d)} \quad (12)$$

$P^F_{t_c}$ is referred to as the Vogel-Czihak-Chang-Wolf (VCCW) fertilisation rate equation (Vogel et al. 1982) and is asymptotically equal to 1 for high sperm concentrations (Gribben et al. 2014). The VCCW equation does not distinguish between mono- and polyspermic fertilisation. This limitation is addressed through the extended-VCCW (EVCCW) equation (Millar & Anderson 2003). The EVCCW equation assumes that an egg becomes polyspermic (nonviable) if additional sperm contact the fertilisable region of a monospermic egg within the time from initial fertilisation to establishment of a block to polyspermy. The formation of a polyspermic block is typically a 2-step process whereby an electrically mediated 'fast' block is rapidly established through depolarisation of the egg membrane which is superseded by a co-occurring 'slow' mechanical and permanent block associated with the cortical reaction — a hardening of the egg fertilisation membrane (Jaffe 1976, Miyazaki & Hirai 1979, Schuel & Schuel 1981, Millar & Anderson 2003). A step function is used to approximate a single complete block where t_B (s) is the time from initial sperm–egg attachment within

the fertilisable zone and establishment of a block to polyspermy (Styan 1998, Millar & Anderson 2003). The time to block establishment (t_B) in *A. planci* is currently unknown; however, in the sea urchin *Strongylocentrotus purpuratus* (Jaffe 1976) and starfishes *Coscinasterias muricata* (Franke 2005) and *Asterina pectinifera* (Miyazaki & Hirai 1979), blocks are established in 0.1 to 1, 0.21, and <1 s, respectively. In the case of *A. pectinifera*, t_B was observed to be as fast as 0.1 s. Consequently, we assume a block establishment of $t_B = 0.2$ s. Monospermic ($P^M_{t_c}$) and polyspermic ($P^P_{t_c}$) fertilisations are expressed through:

$$P^M_{t_c} = \begin{cases} x(t_c)e^{-x(t_c)},\ t_c \le t_B \\ (x(t_c) - x(t_c - t_B)e^{-x(t_c)}) + \\ (e^{-x(t_B)} - e^{-x(t_c)})e^{\beta_0 E_0 t_B},\ t_c > t_B \end{cases} \quad (13)$$

and

$$P^P_{t_c} = 1 - e^{-x(t_c)} - P^M_{t_c} \quad (14)$$

Model tuning

Tuning of the model involved using the VCCW equation (Eq. 12) and varying the plume diffusivity rate (κ) as well as *y*- and *z*-axis diffusion coefficients (α_y and α_z, respectively) to fit measured fertilisation rates (see Box S1 in the Supplement). Parameter values of $\kappa = 0.5$, $\alpha_z = 0.65$, and $\alpha_y = 1.15$ were perturbed to tune the model. Efforts were concentrated on fitting the model to the rising and falling fertilisation values measured lateral to the primary axis of gamete movement (4 and 8 m lateral) to better characterise plume spread. Values of $\kappa = 0.55$, $\alpha_z = 0.51$, and $\alpha_y = 8.61$ were found to best describe plume shape and match empirical fertilisation rates (see Fig. S2).

Advection of fertilised eggs and adhered sperm

The simple coupling of a diffusion and fertilisation kinetics model fails to incorporate that a proportion of eggs downstream of a spawner may have already been fertilised before arriving at a certain point (Lauzon-Guay & Scheibling 2007). The same is true for sperm lost due to adhesion to eggs. To calculate the distribution of viable gametes, lost gametes are subtracted from downstream concentrations (Lauzon-Guay & Scheibling 2007). This process is recursively conducted for each vertical slab (*y*–*z* plane by downstream resolution distance) beginning with the slab immediately downstream of the upper model boundary (i.e. the second slab). The initial slab receives no gametes from upstream and concentrations are therefore a function of the aggregation and plume models. However, fertilisations and sperm adhesions occurring in the first slab do affect downstream concentrations. The movement of lost gametes is modelled through horizontal advection to the cell immediately downstream of their current location (laminar flow). The algorithm for computing the distribution of viable gametes is as follows.

First, we explicitly consider the reduction of sperm due to adhesion to eggs regardless of the egg's fertilised status (Don Ottavio model of fertilisation). Hence we estimate the reduction of sperm, $S_{Reduction}$ (Eq. 10), through the initial egg concentration predicted by the aggregation and diffusion models. That is, in Eq. 10, E_0 equals the egg concentration at each cubic vertex prior to the computation of any fertilisations. This calculates the distribution of free sperm available for egg interactions. Secondly, we calculate the number of egg fertilisations occurring within a slab (mono- and polyspermic) given the free sperm distribution. The reduction of eggs, $P^F_{t_c}$ (Eq. 12), is the total number of fertilisations at a location and is computed using the locations with availability of free sperm (i.e. sperm concentration once the loss of sperm due to possible adhesions in the immediate upstream slab have been subtracted from the current slab). Hence, in Eq. 12, let S_0 equal the free sperm concentration at each cubic vertex at the start of each time step, Δt. This procedure is repeated for every slab in the direction of current excluding the first slab.

Model implementation

We model zygote production and fertilisation rates within 200 m of spawning individuals. Observations of *A. planci* spawnings quantify a total spawning duration of 45 min (Babcock et al. 1994, Benzie et al. 1994). Here, we model spawning at steady state for a period of 30 min (1800 s). This amounts to the summation of 431 Δt time elements ($431 \times 4.17 \approx 1800$ s). It is assumed that plume steady state evolution and dissipation transpires during the non-observed 15 min of spawning. All cohorts of gametes are followed as they advect downstream during the period of observation or until they are lost through the lower boundary. Thus, we follow gametes spawned within the focal region for <14 min and those towards the upper boundary of the total model configuration for ~30 min. All monospermic fertilisations occurring within boundaries of the model focal region are recorded.

Zygote production is calculated as a function of the monospermic fertilisation success and number of eggs at each cubic vertex point (x,y,z) within the model focal region. The temporally cumulative zygote production, Z, at the point (x,y,z) is quantified by:

$$Z(x,y,z) = P^{M}_{t_c}(x,y,z)\, E(x,y,z) \quad (15)$$

where $P^{M}_{t_c}$ and E are the monospermic proportion of eggs fertilised at the point (x,y,z) over the temporal domain (Eq. 13) and egg concentration (Eq. 6) at the point, respectively. To quantify the overall number of zygotes produced at the population level, the production within the bounds of the focal region is summed. Zygote numbers are then averaged across simulations for a given starfish density. This allows production to be considered as a function of population density and aggregation. Similarly, the monospermic and polyspermic fertilisations of a population are obtained by dividing the number of monospermic and polyspermic eggs by the total number of eggs spawned.

A. planci reproductive success was modelled as a function of population density over the range of 0 to 50 starfish ha^{-1}. This density range encompasses the 10 starfish ha^{-1} threshold above which coral cover depletion is likely to occur (Keesing & Lucas 1992). At each density, results were averaged over 350 simulations.

Reproductive success was subsequently considered exclusively as a function of aggregation by fixing the population density. In order to generate differing levels of aggregation, the cluster proportionality constant (α) was fixed at 0.15 whilst the cluster-density proportionality constant ($\beta^{\star}$) was incremented over the interval 0 (randomly distributed) to 1 (highly aggregated). For each aggregation regime (i.e. for each α and $\beta^{\star}$), results were averaged over 350 simulations. Average nearest neighbour distances were calculated from nearest neighbour indices for key aggregation levels. Furthermore, *in situ* variance to mean ratio measurements of *A. planci* population aggregations (Babcock et al. 1994) were approximated by nearest neighbour analysis. This was achieved through running both spatial measures for the same aggregation regimes with each approximation averaged over 5000 simulations (see Table S1 in the Supplement). Nearest neighbour distances and *in situ* approximations were compared with model results. The sensitivity of the model was tested to sex ratio (Fig. S3), mean population diameter (ξ in mm; Fig. S4), mean current velocity (U in m s^{-1}; Fig. S5), and cluster proportionality constant (α; Fig. S6).

RESULTS

Zygote production

Population-level recruitment of *Acanthaster planci* zygotes is predicted by the model to increase with density at a greater than linear rate (concaved upwards). Increased upward concavity of the recruitment curve was observed through comparison with a linear reference line (Fig. 1a) regardless of level of aggregation. Below ~10 starfish ha^{-1}, zygote production was relatively independent of spatial aggregation, yet above this threshold maximal zygote production was achieved through slightly aggregated distributions ($0.15 \leq R < 0.5$). Random distributions resulted in lowest zygote production at all densities. This demonstrates that Allee effects did occur, but they were strongly mediated by aggregation. Somewhat paradoxically, these Allee effects were less pronounced in slightly aggregated populations than for moderate or highly aggregated populations (greater production at high density). In relative terms, for densities >10 starfish ha^{-1}, the production curves of randomly distributed ($0 \leq R < 0.15$), moderately aggregated ($0.5 \leq R < 0.85$), and highly aggregated populations ($0.85 \leq R \leq 1$) yielded similar levels of production which were largely surpassed by the predicted rates within slightly aggregated populations. This is due to increased incidence of polyspermy in moderately and highly aggregated populations and in randomly distributed populations at suboptimal spawner aggregation due to fewer gamete interactions.

Fertilisation success

Comparison of monospermic fertilisation success at different aggregation levels suggests *A. planci* experience greatly increased monospermic fertilisation at <10 starfish ha^{-1} when spawning is highly aggregated and slightly aggregated above this threshold when compared to randomly distributed populations (Fig. 1b). Fertilisation curves were upwardly convex for individuals aggregated at all levels ($0 \leq R \leq 1$). Tighter aggregations increased monospermic fertilisation rates through greater slope at the origin. However, the monospermic fertilisation curve of slight aggregations indicated stronger upward convexity when compared with greater or lesser levels of aggregation across the simulated density range. The positive relationship between increased aggregation and increased curve slope at the origin led to mono-

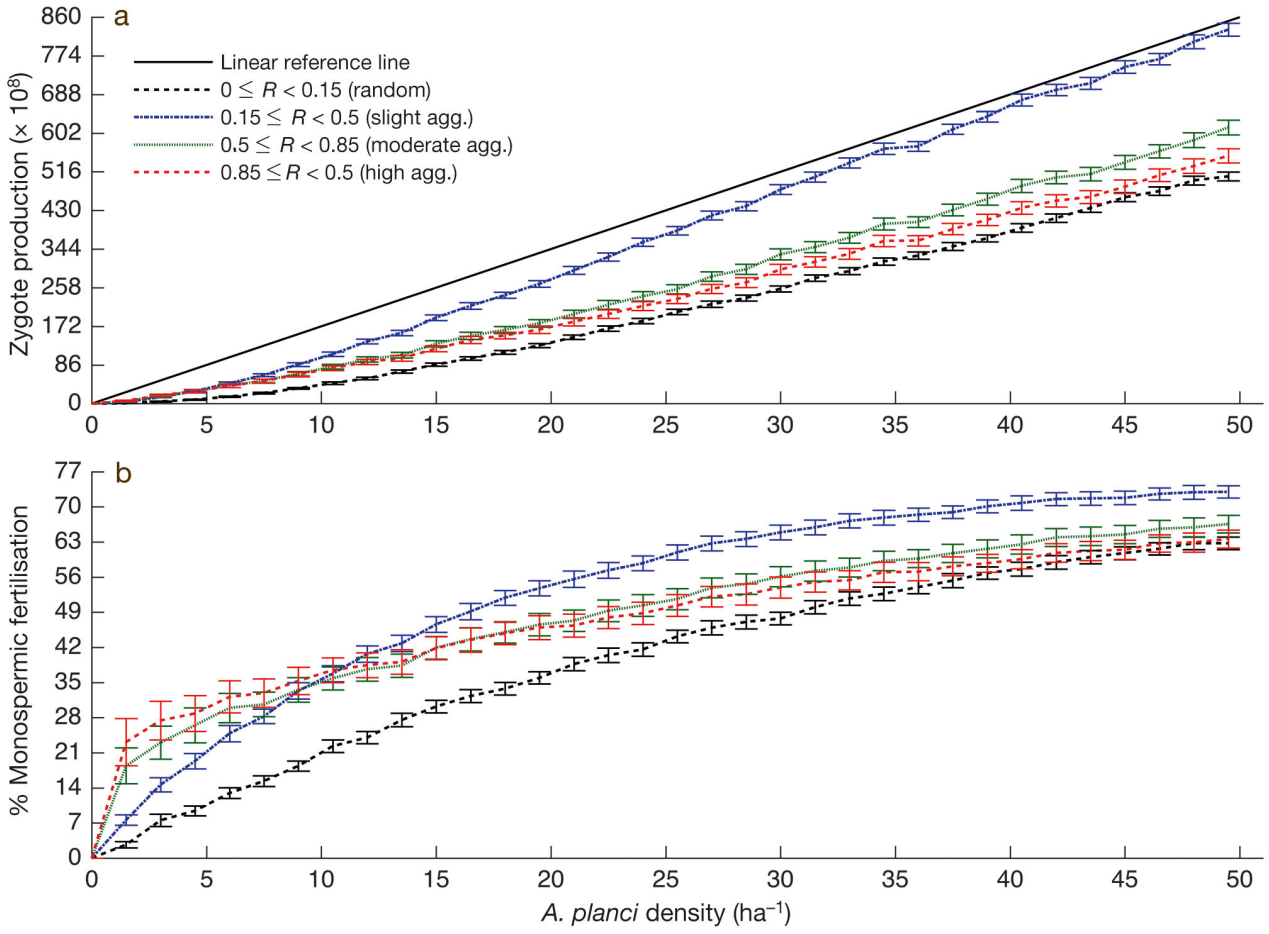

Fig. 1. Predicted *Acanthaster planci* reproductive success for random ($0 \leq R < 0.15$: $\alpha = 0.15$, $\beta^\star = 1$), slightly aggregated ($0.15 \leq R < 0.5$: $\alpha = 0.15$, $\beta^\star = 0.4$), moderately aggregated ($0.5 \leq R < 0.85$: $\alpha = 0.15$, $\beta^\star = 0.1$), and highly aggregated ($0.85 \leq R \leq 1$: $\alpha = 0.15$, $\beta^\star = 0.05$) spatial realisations for (a) population zygote production (±95% CI) versus density over the range 0 to 50 starfish ha^{-1} compared to a linear reference line (not 100% monospermic fertilisation), and (b) % monospermic fertilisation success (±95% CI) versus density over the range 0 to 50 starfish ha^{-1}. Model parameters were $D = 7$ m, $T_s = 2700$ s, $U = 0.12$ m s^{-1} ($\Delta t = 4.17$ s), $h = 0.5$ m, $\kappa = 0.55$, $\alpha_y = 8.61$, $\alpha_z = 0.51$, $P_s = 0.68$, $\xi = 345$ mm, an even sex ratio and results averaged over 350 simulations

spermic fertilisation rates that varied substantially across the different levels of aggregation. At 3 starfish ha^{-1} this culminated in rates increasing from 7.54% for random distributions to 27.43% for highly aggregated. For moderately and highly aggregated individuals, monospermic fertilisation success increased rapidly at densities below a threshold of 3 starfish ha^{-1}. Random spatial distributions yielding suppressed monospermic fertilisation success was consistent across all densities.

The greatly enhanced reproductive success experienced in highly aggregated populations at densities <10 starfish ha^{-1} and slightly aggregated populations above this density was corroborated through modelling monospermic fertilisation success as a function of aggregation. Success was considered for fixed population densities of 3, 15, 25, and 40 starfish ha^{-1} (Fig. 2). The use of 3 and 40 starfish ha^{-1} represent the ends of the density spectrum, whilst 15 and 25 starfish ha^{-1} indicate approximate intermediate densities. Modelling fertilisation in this manner demonstrated that monospermic fertilisation increases with increased aggregation at low densities and that at higher densities (≥15 starfish ha^{-1}) there exists an optimal level of aggregation where monospermic fertilisation success is maximised. At densities <15 starfish ha^{-1} monospermic fertilisation increased monotonically as level of aggregation increased with maximum rates attained (though levelling off) at high levels of aggregation (Fig. 2a; $0.85 \leq R \leq 1$). Conversely, across the same density range, minimal rates of monospermic fertilisation occurred when starfish were randomly distributed while the relative benefit of aggregation decayed as population density increased. This resulted in the development of an optimal aggregation level for densities ≥15 starfish

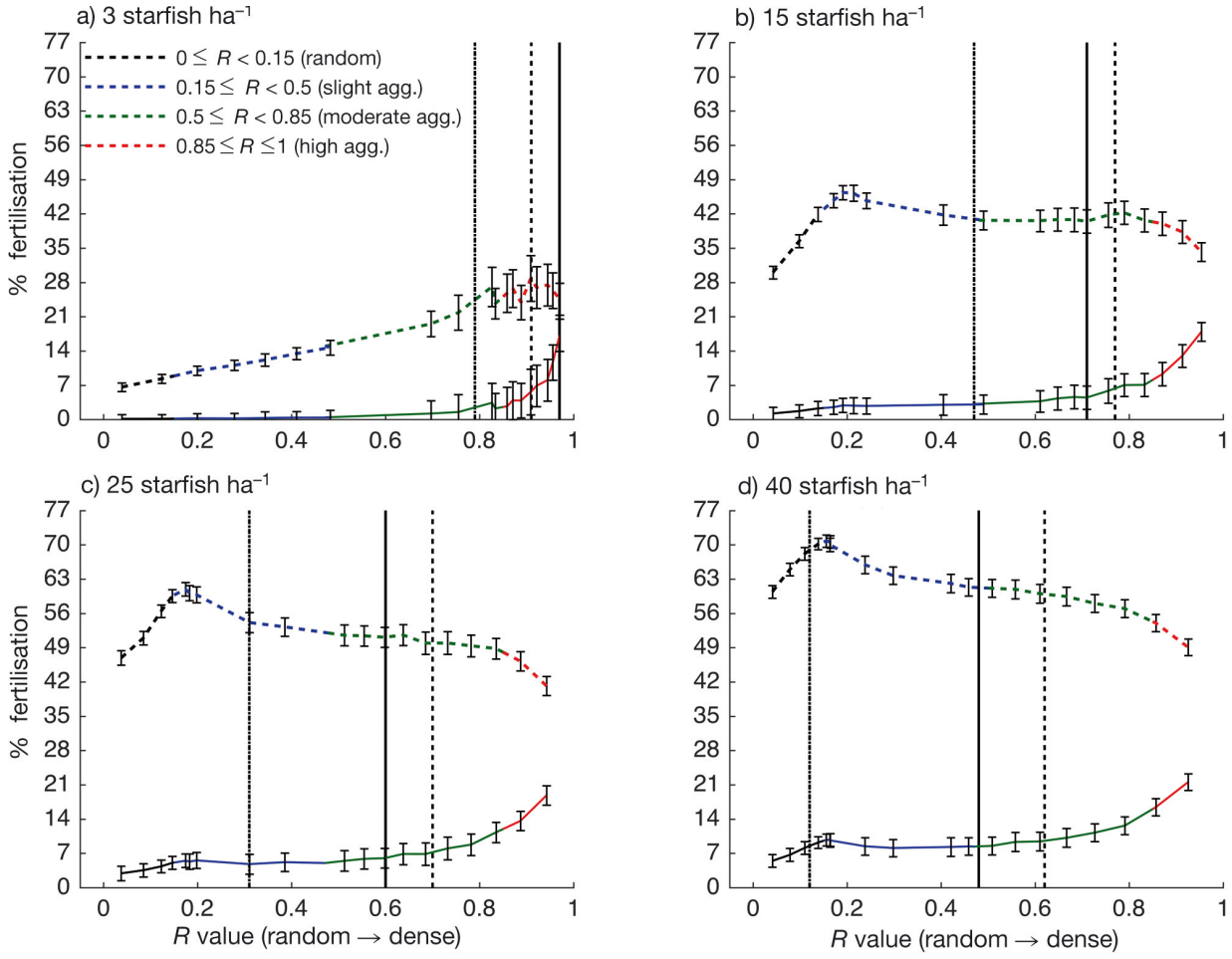

Fig. 2. Predicted fertilisation rates (±95% CI) of *Acanthaster planci* populations as a function of aggregation for fixed densities. Dashed curve: monospermic fertilisation; solid curve: polyspermic fertilisation. Degree of aggregation is measured by modified nearest neighbour analysis (R) for fixed densities of (a) 3, (b) 15, (c) 25, and (d) 40 *A. planci* ha^{-1}. Different aggregations were simulated by incrementing the cluster-density proportionality (β^*) over 0 to 1 for fixed cluster proportionality constant and averaging over 350 simulations for each. Dashed vertical benchmark: approximate nearest neighbour distance of 3 m; dashed-dot vertical benchmark: approximate nearest neighbour distance of 7 m; solid vertical benchmark: approximates *in situ* aggregation measures during a large spawning (88 of 129 individuals) at Davies Reef during summer 1990 to 1991 (VMR = 3.05; Babcock et al. 1994). All 129 starfish were assumed to be distributed within the 6 ha giving a density of 21.5 *A. planci* ha^{-1}. Smaller observed spawnings (≤8 individuals) were more densely aggregated (right of solid benchmark). Model parameters were $D = 7$ m, $T_s = 2700$ s, $U = 0.12$ m s^{-1} ($\Delta t = 4.17$ s), $h = 0.5$ m, $\kappa = 0.55$, $\alpha_y = 8.61$, $\alpha_z = 0.51$, $P_s = 0.68$, $\xi = 345$ mm, an even sex ratio and results averaged over 350 simulations

ha^{-1}. This was such that at population densities ≥15 starfish ha^{-1}, monospermic fertilisation success increased abruptly when aggregation level increased from randomly distributed to slightly aggregated, corresponding to a nearest neighbour index of ~0.2, and decayed as the aggregation level continued to increase (i.e. $R > 0.2$). The rate of decay of aggregative benefit was dependent on population density, which is easily seen through reductions in the slightly-highly aggregated monospermic fertilisation rates: 12.17% at 15 starfish ha^{-1}, 19.74% at 25 starfish ha^{-1}, and 21.73% at 40 starfish ha^{-1} (Fig. 2b,c). Over the same aggregation ranges, polyspermic fertilisation increased by 15.03% at 15 starfish ha^{-1}, 13.34% at 25 starfish ha^{-1} and 11.82% at 40 starfish ha^{-1}. At a nearest neighbour index of ~0.2 for densities >15 starfish ha^{-1}, the post optimal decay of monospermic fertilisation was not found to be a result of increased polyspermic fertilisation — it did not increase when monospermy decreased. This implies that total fertilisation (monospermic fertilisation plus polyspermic fertilisations) was optimal at this aggregation level. Furthermore, variability increased with aggregation level (largest at high levels) and/or decreased population density (largest at lower densities).

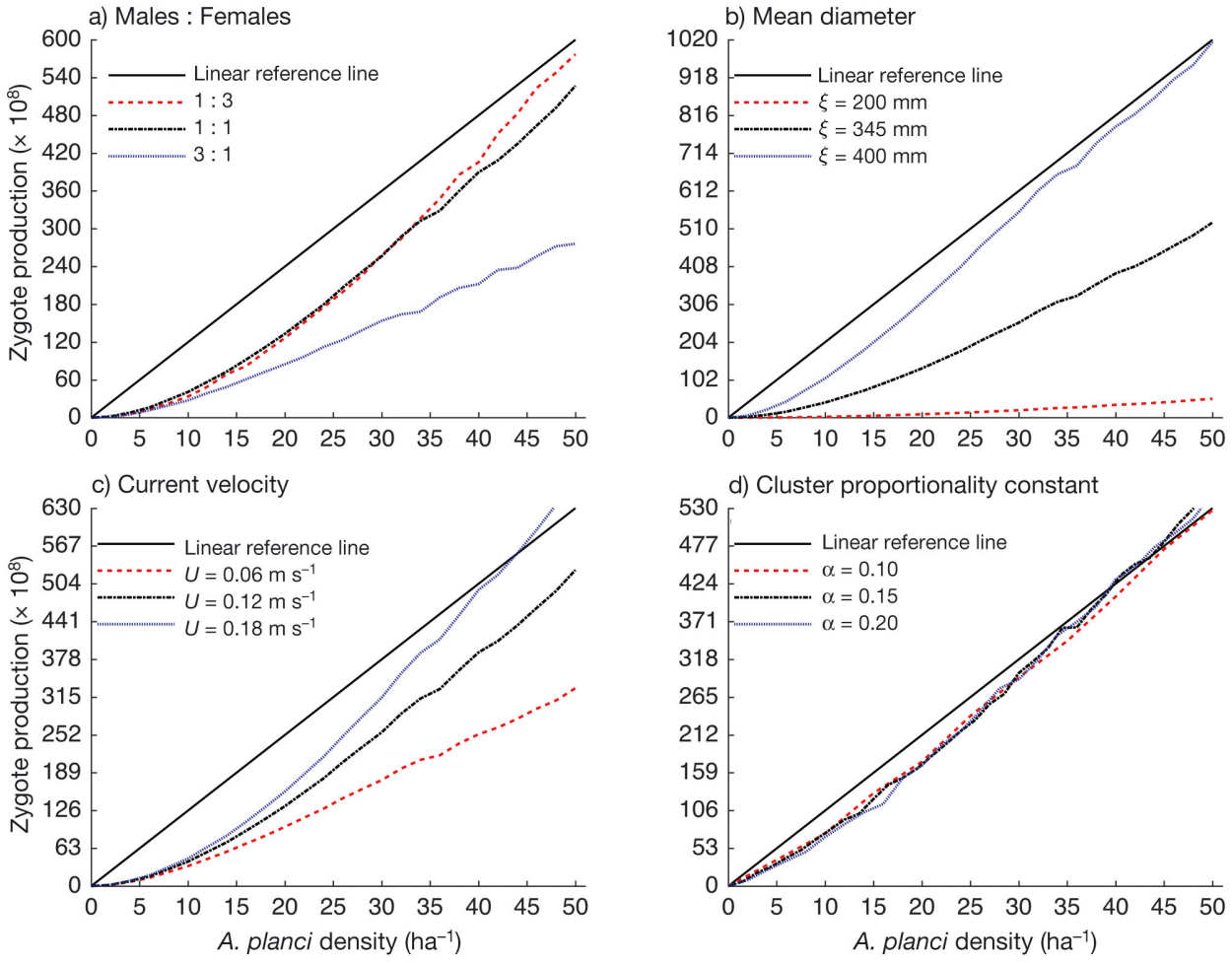

Fig. 3. Sensitivity of *Acanthaster planci* total zygote production versus population density to (a) sex ratio (males to females 0.25, 0.5, 0.75), (b) mean population diameter (ξ = 200, 345, 400 mm) (c) mean current velocity (U = 0.06 [Δt = 8.33 s], 0.12 [Δt = 4.17 s], 0.18 [Δt = 2.78 s] m s^{-1}), and (d) cluster proportionality constant (α = 0.10, 0.15, 0.20; β^* fixed at 0.05). Parameter base rates were D = 7 m, T_s = 2700 s, U = 0.12 m s^{-1} (Δt = 4.17 s), h = 0.5 m, κ = 0.55, α_y = 8.61, α_z = 0.51, P_s = 0.68, ξ = 345 mm, an even sex ratio and results averaged over 350 simulations. Parameters tested for sensitivity were varied

Sensitivity analysis

The model was found to be moderately sensitive to population sex ratio (Fig. 3a), highly sensitive to mean *A. planci* population diameter (Fig. 3b), and slightly sensitive to current velocity (Fig. 3c). Sex ratios favouring males (3:1 ratio) led to reduced zygote production compared to even and female-skewed sex ratios (1:1 and 1:3; Fig. 3a). Whilst the production of sex ratios 1:1 and 1:3 were indistinguishable at densities <40 starfish ha^{-1}, populations comprising more females (fewer males) are predicted to produce more zygotes at densities >40 starfish ha^{-1}. Monospermic fertilisation rates increased with the male proportion of the population.

Zygote production and fertilisation rates increased substantially as starfish increased in size from 200 to 345 mm mean diameter and nearly doubled between 345 and 400 mm. The initial growth phase from 200 to 345 mm spans a period of ~3 yr (2 to 5 yr of age; Pratchett et al. 2014). Increased zygote production associated with greater diameter became conspicuous at ~8 starfish ha^{-1}. Higher zygote production associated with larger starfish is reflected in drastically reduced fertilisation rates as *A. planci* maximal diameter decreased. In general, the model demonstrated positive correlation between increased size and far greater reproductive success. The model was sensitive to the mean current velocity through slightly increased zygote production at faster current velocities and increased monospermic fertilisation rates at slower mean velocities. This anomaly is likely a consequence of a greater quantity of gametes passing through the focal area (with all fertilisations

recorded) as opposed to increased zygote production relative to other mean current velocities. The model was not sensitive to the cluster proportionality constant (Fig. 3d).

DISCUSSION

Modelled spawning populations of *Acanthaster planci*, conditioned on empirical data, were found to be subject to Allee dynamics which manifested through the suppression of individual and population reproductive capacity at low population densities. This spatially explicit, empirically-based fertilisation model showed that aggregative behaviour increased reproductive success at low abundance — an Allee mechanism and potential outbreak catalyst. The stock-recruitment curve demonstrated upward concavity across all simulated densities (0 to 50 starfish ha^{-1}) and spatial distributions (random to highly aggregated) with slight aggregation ($0.15 < R \leq 0.5$) greatly increasing zygote production. In terms of monospermic fertilisation, aggregation produced greater slope near the monospermic fertilisation curve origin. This was corroborated by showing monospermic fertilisation rates increased with aggregation at low population densities (3 starfish ha^{-1}; fixed). However, aggregative benefit, in terms of monospermic fertilisation rates, was found to decay as population density increased (≥15 starfish ha^{-1}). The decay of aggregative benefit occurred through the development of a clearly defined optimal aggregation range ($0.15 \leq R \leq 0.3$) which maximised monospermic fertilisation at slight levels of aggregation, implying aggregation is particularly important at low densities (≤3 starfish ha^{-1}), and that higher levels of aggregation incurred potentially substantial costs in terms of polyspermic fertilisation. Comparison of the model results to *in situ* observations of spawning populations suggest *A. planci* may actually aggregate at or near optimally at low and high densities. Nearest neighbour index approximations (Table S1 in the Supplement) of *in situ* variance to mean ratios observed during natural spawnings (Babcock et al. 1994) indicate high aggregative behaviour for population densities ≤3 starfish ha^{-1} and slight to moderate aggregative behaviour of *A. planci* for densities ≥15 starfish ha^{-1}. Furthermore, model sensitivity indicates monospermic fertilisation rates and zygote production greatly increases with mean starfish diameter from 200 to 345 mm — a growth time frame of ~3 yr.

Zygote production

Modelling of zygote production for *A. planci* populations as a function of density demonstrated that total zygote production accelerates as population size increases (i.e. an Allee effect). Existence of an upwardly concave stock-recruitment curve indicates that if management can reduce a population's density, then reproduction becomes relatively less successful and reduces the risk of an extensive increase in population numbers (i.e. an outbreak). This is important since not all modelling attempts to investigate Allee effects have found evidence for it (e.g. Claereboudt 1999, Lundquist & Botsford 2004). Such studies, for example, investigated the reproductive dynamics of *Strongylocentrotus droebachiensis* (sea urchin; Lundquist & Botsford 2004) and *Placopecten magellanicus* (sea scallop; Claereboudt 1999). While the models of Lundquist & Botsford (2004) and Claereboudt (1999) were similar to the current study, there were key differences. Fundamental differences include the use of different focal species, different spatial scales, omission of boundary conditions incorporating the flow of gametes into their model areas, the preclusion of polyspermic interactions, and using density to estimate zygote production in the case of Lundquist & Botsford (2004). Furthermore, the studies of Lundquist & Botsford (2004) and Claereboudt (1999) were not empirically validated. Our model is tuned to empirical parameters derived from natural and induced *in situ A. planci* spawnings (Babcock et al. 1994, 2014, 2016, R. C. Babcock unpubl. data), integrates potential egg polyspermy, incorporates the effects of boundary conditions and explicitly accounts for the number of monospermic sperm–egg interactions culminating in zygotes. Furthermore, we not only encompassed the flow of fertilised eggs, but also their concentration-specific effect on the availability of free sperm (reductions due to egg adhesion). These aspects may help to explain why this study showed upwardly concave zygote production rather than linear.

Aggregation and Allee dynamics

At low population densities (<3 starfish ha^{-1}) the formation of highly aggregated populations of *A. planci* is model-predicted to vastly improve monospermic fertilisation success and zygote production. However, the degree to which aggregation contributes to increased reproductive success via fertilisation declines as population density increases. It has

been illustrated here that regardless of density, slightly aggregated populations ($0.15 \leq R \leq 0.3$) experience far greater reproductive success than populations with denser or more random spatial distributions. Furthermore, increased aggregation and/or smaller populations induced more variable fertilisation. Various studies have examined the effect of aggregation in the reproduction of free-spawning marine invertebrates (Levitan & Young 1995, Claereboudt 1999, Lundquist & Botsford 2004). Such studies found that aggregating greatly increases population reproductive capacity, particularly at low densities (Claereboudt 1999, Lundquist & Botsford 2004). The current study corroborates markedly increased reproductive capacity — monospermic fertilisation and zygote production — arising from increasingly aggregated spawners at <15 starfish ha^{-1}, however, reproductive optimality tended towards slightly aggregated distributions at densities exceeding this level. That is, at high levels of aggregation polyspermy was found to detrimentally impact monospermic fertilisation when population densities exceeded 15 starfish ha^{-1}.

The results of the model, which show high levels of polyspermic fertilisation under elevated levels of density and aggregation, are consistent with observations such as the evolution of polyspermy blocks in a wide range of free-spawning invertebrates (Schuel & Schuel 1981, Styan 1998), and the fact for *A. planci*, extreme levels of aggregation during spawning have not been observed in nature (Babcock et al. 1994). The sex ratio sensitivity analysis demonstrated zygote production of female-skewed populations were favoured over an even or male-skewed ratio at population densities >35 starfish ha^{-1} (Fig. 3a), indicating polyspermic fertilisations increased with sperm relative to egg concentrations. In comparing slight to dense aggregations, these polyspermic interactions were found to suppress monospermic fertilisation rates by as much as 16.11% at 40 starfish ha^{-1}. These observations lend support to the importance of polyspermy as a selective force in the evolution of a range of behavioural, physiological, and developmental aspects of reproduction in free-spawning marine invertebrates (Levitan 2002, 2004).

There may be more than one underlying reason for this inverse relationship between population density and aggregation density. Models of fertilisation success in another echinoderm, *Clypeaster rosaceus*, also showed negligible aggregative benefits at high population densities (Levitan & Young 1995), even though their model did not account for polyspermy. Models of fertilisation in *Acanthaster* also displayed a post-optimal decay of monospermic fertilisation with aggregation at a given density even allowing for the absence of increased polyspermic fertilisation. Since the fertilisation rate is relative to the concentration and distribution of *A. planci* eggs, we suggest that this optimality indicates a trade-off between the overall coverage and concentration of sperm. This is such that if coverage is maximised then concentration suffers, and if concentration is maximised then coverage suffers. This is consistent with a decreasing aggregative benefit as the random–highly aggregated spectrum compresses.

Persistence of aggregative benefit — albeit at slight aggregation densities — is likely due to the largest simulations of this study comprising no more than 300 individuals (50 starfish ha^{-1} over 6 ha) whereas that of Levitan & Young (1995) for the much smaller *C. rosaceus* considered populations >250 000. Therefore, it is reasonable to assume that this study is consistent with any level of aggregation having a decreasing effect as population density greatly increases, but also extends this to suggest aggregation is ultimately relatively detrimental at high densities. Aggregation-mediated suppression of zygote production alludes to polyspermy as an Allee effect possibly regulating reproduction at large population densities. Increased fertilisation variability associated with increased aggregation and/or smaller populations may be interpreted as greater temporal stochasticity arising from larger between-aggregation distances. Increased distance could reduce chemical communication that is suggested to help synchronise spawnings (Babcock et al. 1994). Based on our finding of reduced variability as population size increases, large and/or high-density populations are likely not to encounter such synchrony problems owing to decreased between-aggregation distances which would improve communication, and consequently, spawning synchrony.

Caveats

The methodology of the current study involves coupling steady-state diffusive gamete plumes with a kinetics model of fertilisation. The primary caveat of this approach stems from the assumption of steady-state and use of a diffusive model and its inability to capture the complexities associated with instantaneous plume structures due to flow disruptions, the rheology and viscosity of mucous strands in which gametes are spawned, and gamete behaviours such as chemotaxis (Crimaldi & Zimmer 2014). These factors may be important in particular situations; how-

ever, the complexities of simulating multiple small scale, non-linear processes are beyond the scope of this model which focuses on larger scale, population-level phenomena. The use of multiple random simulations of plume evolution in our study is useful in this context as it is likely to capture the range of possible variability that may occur mechanistically due to such processes over multiple spawnings.

In situ spawner aggregation and outbreaks

Approximations of *in situ* measures of aggregation provides evidence that large numbers of *A. planci* should optimally display slight to moderate aggregation during spawnings. This indicates increased aggregation likely plays a significant role in outbreak formation. Of the numerous *in situ A. planci* spawning observations, few report spawner spatial distribution, and of those that do, most are qualitative (Pratchett et al. 2014). Quantitative measures of *in situ* aggregation (Babcock et al. 1994) predominantly encompassed small spawnings (≤8 individuals) of highly male-skewed sex ratios (≥0.75) with one large spawning (88 of 129 individuals) of an approximately even male to female ratio (0.57). Parametric and density conditions of the current study mostly reflected the large spawning and were therefore directly compared. Smaller, highly male biased spawnings were indirectly compared. However, *in situ* observations were conducted over 2000 m^2 (200 × 10 m transect; Babcock et al. 1994), whereas the current study assumes distribution over 60000 m^2 (6 ha, 21.5 starfish ha^{-1}). Hence, our results suggest that high density populations of synchronous spawners optimally show slight to moderate aggregation whilst smaller, low density populations should optimally show high levels of aggregation. Such behaviour should reflect an equilibrium between the benefits (e.g. mating success) and the costs (e.g. sperm limitation, polyspermy) as suggested in other free spawners (Levitan & Young 1995). Potential perturbation of a cost-benefit equilibrium by, for example, redistribution of preferred coral prey (Weber & Woodhead 1970, Kenyon & Aeby 2009), would also lead to aggregation and likely aids outbreak formation.

Management options and *A. planci* population modelling into the future

A. planci outbreak management amounts to understanding the regulatory mechanisms of normal abundance (e.g. Dulvy et al. 2004, Fabricius et al. 2010, Wooldridge & Brodie 2015) and, despite aggregation greatly increasing reproductive success, attributing outbreaks to single factor causes is likely to oversimplify the species reproductive dynamics (Pratchett et al. 2014). Yet, characteristics of reefs supporting stable sub-outbreak populations of *A. planci* highlight the importance of mechanisms limiting aggregation, such as coral cover and relative predator abundance (Moore 1990). Early detection and rapid response to incipient outbreak conditions, for example increased optimal/near optimal aggregation and/or density, on a small number of reefs or reef-networks possessing strong larval retention hydrodynamics (leading to build-up of population numbers), presents a feasible management option for preventing or mitigating system-wide outbreaks (Pratchett et al. 2014, Wooldridge & Brodie 2015). The current study quantifies a population density threshold of 3 starfish ha^{-1} for starfish of a mean diameter of 345 mm, based upon aggregation and population density Allee dynamics. Furthermore, sensitivity analysis conducted here implies that fertilisation rates and total zygote production greatly increase in populations with mean size of individuals at diameters between 200 and 345 mm (between 2 and 5 yr post-recruitment), providing ~3 yr to detect and act upon increased abundance as well as highlighting increased outbreak risk of female-skewed populations at higher population density and/or aggregations.

Currently, there are intensive efforts being undertaken in the northern part of the GBR to defend 'high value' tourist destinations and other reefs from an active *A. planci* outbreak. If implemented prior to outbreak initiation, tactics that reduce starfish populations (particularly to <3 starfish ha^{-1}) would limit reproductive potential through decreasing relative recruitment by reducing population density. In addition, they have the potential to further reduce fertilisation and recruitment because larger starfish are more easily detected, and by increasing Allee fertilisation effects through dispersing potential spawners.

While the importance of Allee effects in *A. planci* outbreak formation has been discussed since the 1970s (Dana et al. 1972), evidence to support this Allee theory has been relatively weak. By scaling up previous empirical results (Babcock et al. 1994) to the population level, our work provides the best evidence to date that such effects may be involved in outbreaks. More importantly, we have quantified a threshold level of density and aggregation above which reproductive success will increase dramatically. However, the application of this threshold for

management purposes would be greatly improved by better understanding of *A. planci* polyspermic kinetics, *in situ* spawning behaviour and aggregation. Moreover, the model is sensitive to sex ratios as well as size distribution, both of which are demographic factors that can influence the availability of gametes (e.g. Babcock et al. 1994), which is a key factor in free-spawning success (Levitan & Young 1995, Claereboudt 1999, Lundquist & Botsford 2004). Hence, it would be beneficial to further explore how these factors interact concertedly and in isolation.

Acknowledgements. We thank Anthony Richardson for his guidance and supervision, in addition to supervision by É.E.P., of the honours thesis conducted within the School of Mathematics and Physics at the University of Queensland by J.G.D.R. which formed the basis for this paper. We also thank Alistair Hobday, Scott Condie, and 2 anonymous reviewers who reviewed and made constructive comments which led to improvement of the manuscript. This study builds on earlier research co-funded by the Great Barrier Reef Marine Park Authority (GBRMPA) and CSIRO.

LITERATURE CITED

Babcock RC, Mundy CN (1992) Reproductive biology, spawning and field fertilization rates of *Acanthatser planci.* Mar Freshw Res 43:525–534

Babcock RC, Mundy CN, Whitehead D (1994) Sperm diffusion models and in situ confirmation of long-distance fertilization in the free-spawning asteroid *Acanthaster planci.* Biol Bull (Woods Hole) 186:17–28

Babcock R, Plaganyi ÉE, Morello EB, Rochester W (2014) What are the important thresholds and relationships to inform the management of crown-of-thorns seastar? Final report. CSIRO, Canberra

Babcock R, Milton D, Pratchett M (2016) Relationships between size and reproductive output in the crown-of-thorns starfish. Mar Biol 163:1–7

Baddeley A (2007) Spatial point processes and their applications. In: Weil W (ed) Stochastic geometry: lectures given at the CIME summer school held in Martina Franca, Italy, September 13–18, 2004. Springer, Berlin, p 1–76

Benzie JAH, Dixon P (1994) The effects of sperm concentration, sperm:egg ratio, and gamete age on fertilization success in crown-of-thorns starfish (*Acanthaster planci*) in the laboratory. Biol Bull (Woods Hole) 186:139–152

Benzie JAH, Black KP, Moran PJ, Dixon P (1994) Small-scale dispersion of eggs and sperm of the crown-of-thorns starfish (*Acanthaster planci*) in a shallow coral reef habitat. Biol Bull (Woods Hole) 186:153–167

Birkeland C, Lucas J (1990) *Acanthaster planci*: major management problem of coral reefs. CRC Press, Boca Raton, FL

Brodie J, Fabricius K, De'ath G, Okaji K (2005) Are increased nutrient inputs responsible for more outbreaks of crown-of-thorns starfish? An appraisal of the evidence. Mar Pollut Bull 51:266–278

Claereboudt C (1999) Fertilization success in spatially distributed populations of benthic free-spawners: a simulation model. Ecol Model 121:221–233

Clark PJ, Evans FC (1954) Distance to nearest neighbor as a measure of spatial relationships in populations. Ecology 35:445–453

Crimaldi JP, Zimmer RK (2014) The physics of broadcast spawning in benthic invertebrates. Annu Rev Mar Sci 6: 141–165

Dana TF, Newman WA, Fager EW (1972) *Acanthaster* aggregations: interpreted as primarily responses to natural phenomena. Pac Sci 26:355–372

De'ath G, Fabricius KE, Sweatman H, Puotinen M (2012) The 27–year decline of coral cover on the Great Barrier Reef and its causes. Proc Natl Acad Sci USA 109:17995–17999

Denny MW, Shibata MF (1989) Consequences of surf-zone turbulence for settlement and external fertilization. Am Nat 134:859–889

Dulvy NK, Freckleton RP, Polunin NV (2004) Coral reef cascades and the indirect effects of predator removal by exploitation. Ecol Lett 7:410–416

Fabricius K, Okaji K, De'ath G (2010) Three lines of evidence to link outbreaks of the crown-of-thorns seastar *Acanthaster planci* to the release of larval food limitation. Coral Reefs 29:593–605

Franke ES (2005) Aspects of fertilization ecology in *Evechinus chloroticus* and *Coscinasterias muricata*. PhD dissertation, The University of Auckland

Gribben PE, Millar RB, Jeffs AG (2014) Fertilization success of the New Zealand geoduck, *Panopea zelandica*: effects of sperm concentration, gamete age and contact time. Aquacult Res 45:1380–1388

Hobday AJ, Tegner MJ (2002) The warm and the cold: influence of temperature and fishing on local population dynamics of red abalone. CCOFI Rep 43:74–96

Hobday AJ, Tegner MJ, Haaker PL (2000) Over-exploitation of a broadcast spawning marine invertebrate: decline of the white abalone. Rev Fish Biol Fish 10:493–514

Jaffe LA (1976) Fast block to polyspermy in sea urchin eggs is electrically mediated. Nature 261:68–71

Keesing JK, Lucas JS (1992) Field measurement of feeding and movement rates of the crown-of-thorns starfish *Acanthaster planci* (L.). J Exp Mar Biol Ecol 156: 89–104

Kenyon J, Aeby G (2009) Localized outbreak and feeding preferences of the crown-of-thorns sea star *Acanthaster planci* (Echinodermata, Asteroidea) on reefs off O'ahu, Hawaii. Bull Mar Sci 84:199–209

Kettle B, Lucas J (1987) Biometric relationships between organ indices, fecundity, oxygen consumption and body size in *Acanthaster planci* (L.) (Echinodermata; Asteroidea). Bull Mar Sci 41:541–551

Krebs CJ (1999) Spatial patterns and indices of dispersion. In: Krebs CJ (ed) Ecological methodology. Benjamin Cummings, Menlo Park, CA, p 191–226

Lauzon-Guay JS, Scheibling RE (2007) Importance of spatial population characteristics on the fertilization rates of sea urchins. Biol Bull (Woods Hole) 212:195–205

Levitan DR (2002) Density dependent selection on gamete traits in three congeneric sea urchins. Ecology 83: 464–479

Levitan DR (2004) Density-dependent sexual selection in external fertilizers: variances in male and female fertilization success along the continuum from sperm limitation to sexual conflict in the sea urchin *Strongylocentrotus franciscanus*. Am Nat 164:298–309

Levitan DR, Petersen C (1995) Sperm limitation in the sea. Trends Ecol Evol 10:228–231

Levitan DR, Young CM (1995) Reproductive success in large populations: empirical measures and theoretical predictions of fertilization in the sea biscuit *Clypeaster rosaceus*. J Exp Mar Biol Ecol 190:221–241

Levitan DR, Sewell MA, Chia FS (1991) Kinetics of fertilization in the sea urchin *Strongylocentrotus franciscanus*: interaction of gamete dilution, age, and contact time. Biol Bull (Woods Hole) 181:371–378

Liermann M, Hilborn R (2001) Depensation: evidence, models and implications. Fish Fish 2:33–58

Lundquist CJ, Botsford LW (2004) Model projections of the fishery implications of the Allee effect in broadcast spawners. Ecol Appl 14:929–941

Lundquist CJ, Botsford LW (2010) Estimating larval production of a broadcast spawner: the influence of density, aggregation, and the fertilization Allee effect. Can J Fish Aquat Sci 68:30–42

Millar RB, Anderson MJ (2003) The kinetics of monospermic and polyspermic fertilization in free-spawning marine invertebrates. J Theor Biol 224:79–85

Miyazaki Si, Hirai S (1979) Fast polyspermy block and activation potential: correlated changes during oocyte maturation of a starfish. Dev Biol 70:327–340

Moore RJ (1990) Persistent and transient populations of the crown-of-thorns starfish, *Acanthaster planci*. In: Bradbury R (ed) *Acanthaster* and the coral reef: a theoretical perspective proceedings of a workshop held at the Australian Institute of Marine Science, Townsville, August 6–7, 1988. Springer-Verlag, Berlin, p 236–277

Nakamura M, Okaji K, Higa Y, Yamakawa E, Mitarai S (2014) Spatial and temporal population dynamics of the crown-of-thorns starfish, *Acanthaster planci*, over a 24-year period along the central west coast of Okinawa Island, Japan. Mar Biol 161:2521–2530

Ormond RFG, Campbell AC, Head SH, Moore RJ, Rainbow PR, Saunders AP (1973) Formation and breakdown of aggregations of the crown-of-thorns starfish, *Acanthaster planci* (L.). Nature 246:167–169

Pennington JT (1985) The ecology of fertilization of echinoid eggs: the consequences of sperm dilution, adult aggregation, and synchronous spawning. Biol Bull (Woods Hole) 169:417–430

Pratchett MS (2005) Dynamics of an outbreak population of *Acanthaster planci* at Lizard Island, northern Great Barrier Reef (1995–1999). Coral Reefs 24:453–462

Pratchett MS (2007) Feeding preferences of *Acanthaster planci* (Echinodermata: Asteroidea) under controlled conditions of food availability. Pac Sci 61:113–120

Pratchett MS, Caballes CF, Rivera Posada JA, Sweatman HPA (2014) Limits to understanding and managing outbreaks of crown-of-thorns starfish (*Acanthaster* spp.). Oceanogr Mar Biol Annu Rev 52:133–200

Quinn JF, Wing SR, Botsford LW (1993) Harvest refugia in marine invertebrate fisheries: models and applications to the red sea urchin, *Strongylocentrotus franciscanus*. Am Zool 33:537–550

Schuel H, Schuel R (1981) A rapid sodium-dependent block to polyspermy in sea urchin eggs. Dev Biol 87:249–258

Stierhoff KL, Neuman M, Butler JL (2012) On the road to extinction? Population declines of the endangered white abalone, *Haliotis sorenseni*. Biol Conserv 152:46–52

Stockie JM (2011) The mathematics of atmospheric dispersion modeling. SIAM Rev 53:349–372

Styan CA (1998) Polyspermy, egg size, and the fertilization kinetics of free spawning marine invertebrates. Am Nat 152:290–297

Sweatman H, Delean S, Syms C (2011) Assessing loss of coral cover on Australia's Great Barrier Reef over two decades, with implications for longer-term trends. Coral Reefs 30:521–531

Teruya T, Suenaga K, Koyama T, Nakano Y, Uemura D (2001) Arachidonic acid and α-linolenic acid, feeding attractants for the crown-of-thorns sea star *Acanthaster planci*, from the sea urchin *Toxopneustes pileolus*. J Exp Mar Biol Ecol 266:123–134

Tobin PC, Berec L, Liebhold AM (2011) Exploiting Allee effects for managing biological invasions. Ecol Lett 14: 615–624

Vine PJ (1973) Crown of the thorns (*Acanthaster planci*) plagues: the natural causes theory. Atoll Research Bulletin No. 166, Smithsonian Institution, Washington, DC

Vogel H, Czihak G, Chang P, Wolf W (1982) Fertilization kinetics of sea urchin eggs. Math Biosci 58:189–216

Weber JN, Woodhead PMJ (1970) Ecological studies of the coral predator *Acanthaster planci* in the South Pacific. Mar Biol 6:12–17

Wooldridge SA, Brodie JE (2015) Environmental triggers for primary outbreaks of crown-of-thorns starfish on the Great Barrier Reef, Australia. Mar Pollut Bull 101:805–815

Zannetti P (1990) Gaussian models. In: Zannetti P (ed) Air pollution modeling: theories, computational methods and available software, Book 1. Springer Science + Business Media, New York, NY, p 141–183

Editorial responsibility: Pei-Yuan Qian, Kowloon, Hong Kong SAR

Submitted: September 9, 2016; Accepted: July 6, 2017
Proofs received from author(s): August 22, 2017